Interfacial Ferromagnetism and Exchange Bias in $CaRuO_3/CaMnO_3$ Superlattices

C. He,[1,*] A. J. Grutter,[1,2] M. Gu,[3] N. D. Browning,[3,†] Y. Takamura,[3] B. J. Kirby,[4] J. A. Borchers,[4] J. W. Kim,[5] M. R. Fitzsimmons,[5] X. Zhai,[1,‡] V. V. Mehta,[1,2] F. J. Wong,[1] and Y. Suzuki[1,2,6]

[1]*Department of Materials Science and Engineering, University of California, Berkeley, California 94720, USA*
[2]*Materials Sciences Division, Lawrence Berkeley National Laboratory, Berkeley, California 94720, USA*
[3]*Department of Chemical Engineering and Materials Science, University of California, Davis, California 95616, USA*
[4]*NIST Center for Neutron Research, National Institute of Standards and Technology, Gaithersburg, Maryland 20899, USA*
[5]*Los Alamos National Laboratory, Los Alamos, New Mexico 87545, USA*
[6]*Department of Applied Physics and Geballe Laboratory for Advanced Materials, Stanford University, Stanford, California 94305, USA*

(Received 17 April 2012; revised manuscript received 3 September 2012; published 7 November 2012)

We have found ferromagnetism in epitaxially grown superlattices of $CaRuO_3/CaMnO_3$ that arises in *one unit cell* at the interface. Scanning transmission electron microscopy and electron energy loss spectroscopy indicate that the difference in magnitude of the Mn valence states between the center of the $CaMnO_3$ layer and the interface region is consistent with double exchange interaction among the Mn ions at the interface. Polarized neutron reflectivity and the $CaMnO_3$ thickness dependence of the exchange bias field together indicate that the interfacial ferromagnetism is only limited to one unit cell of $CaMnO_3$ at each interface. The interfacial moment alternates between the $1\mu_B$/interface Mn ion for even $CaMnO_3$ layers and the $0.5\mu_B$/interface Mn ion for odd $CaMnO_3$ layers. This modulation, combined with the exchange bias, suggests the presence of a modulating interlayer coupling between neighboring ferromagnetic interfaces via the antiferromagnetic $CaMnO_3$ layers.

DOI: 10.1103/PhysRevLett.109.197202 PACS numbers: 75.70.Cn, 75.47.Lx

Among a wide spectrum of novel phenomena induced at heterointerfaces, ferromagnetism (FM) generated from two non-FM materials is of interest both from a fundamental perspective and also from potential applications associated with spintronics architecture. Yet only a few examples have been reported in the literature. They include $LaCrO_3/LaFeO_3$ [1] and $(LaMnO_3)_{2n}/(SrMnO_3)_n$ [2] superlattices, where all constituent layers are antiferromagnetic (AFM) insulators. In $LaCrO_3/LaFeO_3$ superlattices [1], $Cr^{3+}(3d^3)$ and $Fe^{3+}(3d^5)$ are FM coupled via oxygen ions as predicted by the Goodenough-Kanamori rules. In $(LaMnO_3)_{2n}/(SrMnO_3)_n$ superlattices, a FM metal is generated in short superlattice period samples ($n < 3$) [2] via a double exchange interaction.

Unlike these examples, $CaRuO_3$ (CRO)/$CaMnO_3$ (CMO) superlattices are composed of a paramagnetic metal (CRO) [3–6] and an AFM insulator (CMO) [7,8]. Interface FM in the superlattices grown on (001) $LaAlO_3$ (LAO) substrates was first illustrated by Takahashi *et al.* [9]. More recent x-ray resonant magnetic scattering (XRMS) studies suggested that FM extends to 3–4 CMO unit cells (u.c.) at interfaces [10]. However, density-functional theory (DFT) calculations indicate that if the interfacial magnetism is attributed to double exchange (DE) at interfaces due to charge transfer from CRO to CMO, the FM should be attributed to one unit cell at the interface [11]. In order to determine whether DE is the mechanism, we must eliminate other possible sources of FM. In both of these studies, superlattices of fixed CMO layer and varied CRO layer were coherently strained to the underlying LAO substrates. Such coherent epitaxial strain can introduce lattice distortions that in turn affect the magnetic ground state of the system. In addition, the effects of alloying at interfaces must be taken into consideration as FM is observed in bulk $CaMn_{1-x}Ru_xO_3$ for x as small as 0.1 [12]. In order to eliminate effects of epitaxial strain and alloying from those of DE due to charge transfer among the Ru and Mn ions, we need to understand how this FM evolves with CMO layer thickness as the CMO layer is thought to be the source of FM signal [11].

In this Letter, we demonstrate that FM in CRO/CMO superlattices is due to a DE mechanism attributed to the leakage of itinerant electrons from CRO to CMO in *one unit cell* (u.c.) at interfaces through exchange bias (EB), polarized neutron reflectivity (PNR), and scanning transmission electron microscopy electron energy loss spectroscopy (EELS) measurements. In contrast to previous experiments, we examined a series of $[(CRO)_3/(CMO)_N]_{10}$ superlattices ($N = 3$–12) on (001) $SrTiO_3$ (STO) substrates where the thickness of the CMO layers was varied while keeping the thickness of the CRO layer fixed. Our first observations of EB directly confirm the existence of strong magnetic coupling between an interfacial FM and a neighboring AFM within the CMO layers. Investigations of EB with varying CMO layer thickness indicate that interfacial FM is limited to one u.c. of CMO at the interfaces as predicted by DFT calculations. Most surprisingly, we discovered that superlattices with even and odd N showed

interfacial Mn moments of $1.0\mu_B$/Mn and $0.5\mu_B$/Mn respectively for $N > 3$. This distribution suggests the possible existence of a modulating coupling between neighboring FM interfaces mediated via the varying AFM CMO layers.

The superlattices of CRO/CMO were grown by pulsed laser deposition with a KrF laser (wavelength of $\lambda =$ 248 nm and laser fluence of 1.6 J/cm^2) at 680 °C and 20 m Torr O_2 on TiO_2-terminated STO (001) substrates. The samples were cooled in 20 m Torr O_2. Superlattices comprised of 10 periods of 3 u.c. of CRO and N u.c. (where $N = 3$–12) of CMO were fabricated. X-ray diffraction (XRD) experiments, in the form of θ-2θ scans, confirmed the epitaxial growth of (001) CMO and CRO layers on (001) STO substrates in all superlattices. Reciprocal space maps (RSM) indicated that the CMO layers were structurally relaxed and assumed lattice parameters close to bulk values [13]. The relaxed growth eliminates possible strain-induced magnetism. The atomic abruptness of the interfaces in the superlattices was probed via x-ray reflectivity (XRR) and transmission electron microscopy (TEM). Figure 1(a) shows a representative XRR scan for a $(CRO)_3/(CMO)_{12}$ superlattice. The low and high frequency oscillations correspond to the superlattice period and the total thickness, respectively. In the sample shown in Fig. 1(a), the total sample thickness of 55.9 nm deduced from the XRR is in agreement with the expected value of 56.3 nm assuming relaxed growth. In an atomic resolution Z-contrast image [Fig. 1(b)], the CRO layers appear brighter due to the localization of the heavy element Ru. A cross sectional energy filtered TEM image at the Mn L edge of a $(CRO)_3/(CMO)_{15}$ superlattice in Fig. 1(c) inset shows that the interfaces are sharp over large areas and throughout the whole thickness of the superlattice with minimal Mn interdiffusion into the CRO layers. Figure 1(c) shows an integrated Mn L edge line scan over the region indicated by the white line A in Fig. 1(b). The scan shows that the interfaces are abrupt without a large amount of Mn interdiffusion into CRO. The Mn L edge EELS [Fig. 1(d)] shows that the L_3/L_2 ratio at the interface is enhanced compared to that in the center of the CMO layer. Quantitative analysis using the L_3/L_2 ratio method [14] determined that the valence state of the Mn ions in the center of the CMO layer is around 3.9 compared to about 3.8 in the interface region. The deviation of the Mn valence away from the expected value of 4+ in the center of the CMO sublayer may be due to the systematic error bar $\sim \pm 0.15$ of this method [14]. In any case, the magnitude of the valence state difference between the center of the CMO layer and the interface region is consistent with the calculated electron leakage with DFT calculations [11].

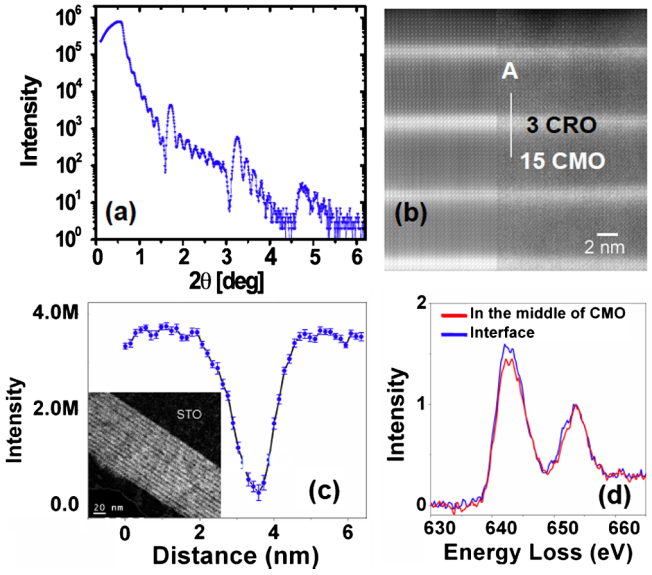

FIG. 1 (color online). (a) X-ray reflectivity scan of $(CRO)_3/(CMO)_{12}$, (b) cross sectional atomic resolution Z-contrast TEM image of $(CRO)_3/(CMO)_{15}$ (the left half of the image is noise reduced using the principle component analysis), (c) integrated Mn L edge intensity across the interface along the white line A in (b) with an energy integration window 640–660 eV and (d) EELS spectra obtained from the CMO region and the CMO/CRO interface region. The EELS spectra were normalized to the L_2 peak maximum. Inset of (c): Mn energy filtered TEM of $(CRO)_3/(CMO)_{15}$.

To directly probe the interfacial magnetic profile with polarization analysis, we performed PNR experiments on $N = 10$ and $N = 11$ superlattices. For the $N = 10$ sample, a polarized neutron beam was incident on the sample with propagation direction perpendicular to the magnetic field H and the sample surface, and the specular reflectivity was measured as a function of wave vector transfer along the surface normal Q_z. Polarization analysis of the scattered beam revealed no spin-flip scattering; thus, we refer only to the spin-up and spin-down non-spin-flip cross sections. For this scattering geometry, the spin-up and spin-down non-spin-flip reflectivities are functions of the depth profiles $\rho(z)$, the nuclear scattering length density, and $M(z)$, the magnetization component parallel to H. The magnetic profile was deduced via modeling of polarized beam data taken after the sample had been cooled to 5 K in 0.82 T [15]. Figure 2(a) shows the fitted non-spin-flip PNR data for the $N = 10$ superlattice plotted as Fresnel reflectivity (reflectivity scaled by the theoretical reflectivity of the bare STO substrate). The salient features of the spectra are the low Q_z oscillatory spin splitting, and the spin splitting of the first-order superlattice Bragg peak near $Q_z \sim 1.4$ nm^{-1}. The data are well fit by a model where FM is assumed to arise solely from one u.c. of interfacial CMO, as shown in Figs. 2(b) and 2(c). This solution is not unique, as models featuring 2 magnetized u.c. of interfacial CMO, or uniformly magnetized CRO yield qualitatively similar fits to the data. However, we can strictly rule out other competing models, including those featuring magnetic moment that arises from a uniformly magnetized superlattice and uniformly magnetized CMO layers. These

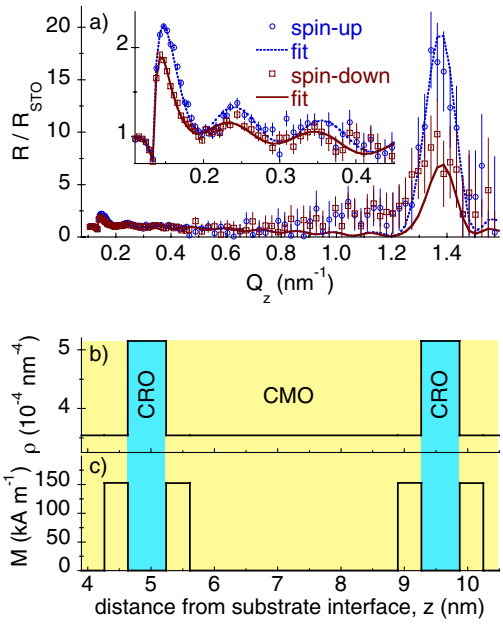

FIG. 2 (color online). (a) PNR spectra for $(CRO)_3/(CMO)_{10}$ measured at 5 K in 0.82 T after field cooling. Inset highlights low- Q_z scattering. (b) Nuclear depth profile. (c) Magnetic depth profile corresponding to 1 u.c. interfacial CMO magnetization.

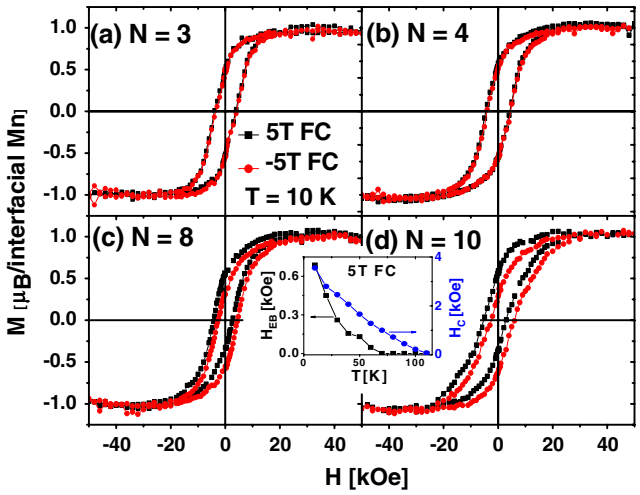

FIG. 3 (color online). Field dependence of magnetization of $(CRO)_3/(CMO)_N$ superlattices at $T = 10$ K for (a) $N = 3$, (b) $N = 4$, (c) $N = 8$, and (d) $N = 10$. The measurements are done after 5 T (black squares) and -5 T (red circles) field cooling respectively from 300 K. Inset of (c) and (d) shows T dependence of H_C and H_{EB} for $(CRO)_3/(CMO)_8$.

models cannot reproduce the spin dependence of the Bragg peak and the spin splitting at low Q_z. Therefore, the PNR data are consistent with magnetic moment arising from 1 u.c. of CMO at the CMO/CRO interfaces, and conclusively confirm a periodic distribution of moment.

Similar PNR measurements performed for the $N = 11$ sample are also consistent with a magnetization distribution that is localized at the CMO interfaces. We note that for both the $N = 10$ and $N = 11$ samples, the PNR measurements cannot distinguish between symmetric magnetization profiles (Fig. 2), and profiles in which the magnetization of one CMO interface layer is nonmagnetic or weakly magnetized and the other CMO interface layer is more strongly magnetized. However, PNR does not indicate a magnetic profile of one FM unit cell for N odd and two FM unit cells for N even at one interface and no FM at the other.

Figure 3 shows the hysteresis loops of four representative samples ($N = 3, 4, 8, 10$) at $T = 10$ K. The measurements were performed after field cooling from 300 K in a ± 5 T field. For all these superlattices, the saturation magnetization ($M_S \sim 1.0\mu_B$/interfacial Mn) is independent of cooling field. For the $N = 3$ superlattice [Fig. 3(a)], the two loops are basically the same with both centered around zero field. For the $N = 4$ superlattice [Fig. 3(b)], the hysteresis loops cooled in ± 5 T are no longer centered around zero field and are clearly shifted by ∓ 0.018 T, respectively. These shifts in the hysteresis loops are indicative of EB phenomena. EB was first discovered by Meiklejohn and Bean [16] and is most often observed in systems containing FM-AFM interfaces where the AFM layer acts to effectively bias the FM layer. Such a unidirectional anisotropy is influenced by many factors, such as interface roughness, FM layer thickness, AFM layer thickness, interface spin structures etc. [17,18]. For superlattices with $N = 8$ [Fig. 3(c)] and $N = 10$ [Fig. 3(d)], the exchange bias field (H_{EB}) increases to 0.09 and 0.12 T, respectively. The observation of EB in the CRO/CMO superlattice is strong evidence that there is a FM layer strongly magnetically coupled to an adjacent AFM layer. The onset of EB in the $N = 4$ superlattice indicates the presence of AFM ordering in the 4 CMO layers. If at least 2 u.c. of CMO is necessary to form AFM ordering, then there could only be one u.c. of FM CMO layer at each interface in the $N = 4$ superlattice. For the $N = 8$ and 10 superlattices, H_{EB} increases due to the increased pinning force from thicker adjacent AFM CMO layers. However, the value of M_S is similar to the $N = 4$ superlattice, indicating that the number of FM layers at each interface is similar to $N = 4$, i.e., one u.c. The independence of M_S on CMO layer thickness suggests that interdiffusion is not the primary cause for FM behavior in CRO/CMO superlattices. The reason is that the interdiffusion volume in superlattices with thicker CMO layers is expected to increase due to rougher interfaces, thus resulting in larger M_S. In addition, we believe that FM due to oxygen deficiency, as reported in $CaMnO_{3-\delta}$ nanoparticles [19] could not explain the FM observed in the CRO/CMO superlattices. FM due to oxygen deficiency gives rise to much smaller M_S and should be directly proportional to the CMO volume—both of which are inconsistent with our observations.

To understand the origin of EB in these superlattices we examined its temperature dependence. The inset in Figs. 3(c) and 3(d) shows the temperature dependence

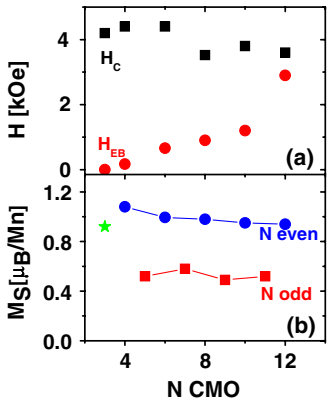

FIG. 4 (color online). CMO thickness dependence of (a) H_{EB} and H_C and (b) M_S in the superlattices.

of H_{EB} for the $N = 8$ superlattice. With increasing temperature, H_{EB} monotonically decreases and vanishes around 70 K, thus indicating a blocking temperature of $T_B \sim 70$ K, which is smaller than the Neél temperature ($T_N \sim 120$ K) of the CMO layer. The fact that $T_B < T_N$ strongly suggests that EB observed in CRO/CMO depends on the existence of AFM ordering in the CMO layers. H_C approaches zero around 110 K which is T_C determined from $M(T)$ [13].

We also studied the evolution of H_{EB} as well as H_C as a function of CMO layer thickness, as shown in Fig. 4(a). H_C remains constant at about 0.35 T for all N shown, thus suggesting that the FM layer does not change much from superlattice to superlattice and is consistent with interfacial FM. H_{EB}, however, increases monotonically with increasing N. Such a trend is consistent with the materials dependent behavior of conventional FM/AFM bilayers in the limit of low AFM thickness [17,18]. The higher H_{EB} is attributed to increased pinning force exerted by thicker AFM films, which, in our case, is the CMO layer minus the interfacial FM layers within a superlattice period. The failure to observe saturation of H_{EB} at large N is possibly due to the relatively small thickness of the CMO layer even for the largest N in our study. It is worthwhile to reiterate that the onset of H_{EB} occurs at $N = 4$, so that we may describe the CMO layers in superlattices with $N \geq 4$ to be composed of the core AFM layers sandwiched by one u.c. of interfacial FM layer on each side. The $N = 3$ case is a special one where there is only one u.c. of noninterfacial CMO layer. We believe this one layer to be insufficient to produce AFM ordering, thus resulting in the absence of EB.

We also investigated M_S as a function of CMO layer thickness N. For superlattices with $N = 4, 6, 8, 10, 12$, the values were all about $1.0\mu_B$/interfacial Mn ion. In excellent agreement with the PNR spectra, for odd values of $N = 5, 7, 9, 11$, M_S is consistently smaller and about $0.5\mu_B$/interfacial Mn ion. The differences in M_S values are clearly illustrated in Fig. 4(b). For the $N = 3$ superlattice, the one u.c. of non-interfacial CMO layer may add to the interfacial FM signal, thus making it qualitatively similar to even N superlattices. With the exception of the $N = 3$ superlattice, the M_S values fall into two categories: $\sim 1.0\mu_B$/Mn for even CMO layers and $\sim 0.5\mu_B$/Mn for odd CMO layers. One would expect that for the odd N superlattices, neighboring FM layers should have a parallel magnetic configuration via nearest neighbor interactions through adjacent AFM layers, thus leading to the constructive addition of FM signal; for the even N superlattices, we would expect neighboring FM layers to have an anti-parallel magnetic configuration, thus resulting in zero M_S. However, our observations seem to indicate that there exists some type of modulating coupling mechanism between nearest neighboring FM layers mediated via insulating AFM CMO layers that is a maximum for even N CMO layers and is a minimum for odd N CMO layers. We have found that M_S is independent of CRO layer thickness (data not shown here). Therefore, it is difficult to believe that the coupling originates from the metallic CRO layers. However, spin polarization is likely induced to a certain degree in the itinerant electrons in the CRO. Another factor that needs to be taken into account is the asymmetry of the interfaces, possibly resulting in dissimilar neighboring FM layers. In fact, TEM shows that interfaces with an underlying CRO are smoother than those with an underlying CMO layer. However such structural differences alone cannot explain the magnetization of N odd versus N even superlattices. Furthermore, we cannot rule out the possibility of differing amounts of electron leakage from CRO to CMO between $N =$ odd and $N =$ even samples. In any case, more theoretical work needs to be carried out to probe the mechanism responsible for oscillatory magnetization as a function of CMO layer thickness.

In summary, we have found ferromagnetism in $(CRO)_3/(CMO)_N$ superlattices on STO (001) substrates whose interfacial moment value is constrained to *one unit cell* in agreement with DFT calculations that attributes the FM to DE at interfaces due to charge transfer from CRO to CMO. STEM EELS indicates that the difference in magnitude of Mn valence states between the center of the CMO layer and the interface region is consistent with DE at interfaces. PNR and the CMO thickness dependence of EB field together indicate that interfacial FM is only limited to one u.c. of CMO at each interface. Remarkably, we found that the even and odd N superlattices possess strikingly different M_S at interfaces, $\sim 1.0\mu_B$/Mn and $\sim 0.5\mu_B$/Mn, respectively, for $N > 3$. Such a remarkable difference may be attributed to a modulating coupling mechanism between nearest FM layers as a function CMO layer thickness.

We would like to thank Professor Michael Flatté and Professor Robert M. White for fruitful discussions. C. H. was supported by the Army Research Office MURI-W911 NF-08-1-0317. A. J. G., V. V. M., and the TEM work performed at NCEM were supported by the Director, Office of Science, Office of Basic Energy Sciences, of the U.S.

Department of Energy (DOE) (DE-AC02-05CH11231). The TEM work at UC Davis was supported by the National Science Foundation (DMR-747896) and by the Office of Science, Office of Basic Energy Sciences of the U.S. DOE (DE-FG0203ER46057). Los Alamos National Laboratory is operated by Los Alamos National Security LLC under DOE Contract No. DE-AC52-06NA25396.

*chunyong.he@gmail.com

†Present address: Fundamental and Computational Sciences Directorate, Pacific Northwest National Laboratory, Richland, WA 99352, USA.

‡Present address: Hefei National Laboratory for Physical Sciences at the Microscale, University of Science and Technology, China.

[1] K. Ueda, H. Tabata, and T. Kawai, Science **280**, 1064 (1998).

[2] A. Bhattacharya, S. May, S. te Velthuis, M. Warusawithana, X. Zhai, B. Jiang, J.-M. Zuo, M. Fitzsimmons, S. Bader, and J. Eckstein, Phys. Rev. Lett. **100**, 257203 (2008); C. Adamo, X. Ke, P. Schiffer, A. Soukiassian, M. Warusawithana, L. Maritato, and D. G. Schlom, Appl. Phys. Lett. **92**, 112508 (2008).

[3] S. Kamal, D. M. Kim, C. B. Eom, and J. S. Dodge, Phys. Rev. B **74**, 165115 (2006).

[4] Y. S. Lee, J. Yu, J. Lee, T. Noh, T.-H. Gimm, H.-Y. Choi, and C. B. Eom, Phys. Rev. B **66**, 041104 (2002).

[5] I. I. Mazin and D. J. Singh, Phys. Rev. B **56**, 2556 (1997).

[6] G. L. Catchen, T. M. Rearick, and D. G. Schlom, Phys. Rev. B **49**, 318 (1994).

[7] J. J. Neumeier and J. L. Cohn, Phys. Rev. B **61**, 14319 (2000).

[8] E. O. Wollan and W. C. Koehler, Phys. Rev. **100**, 545 (1955).

[9] K. S. Takahashi, M. Kawasaki, and Y. Tokura, Appl. Phys. Lett. **79**, 1324 (2001).

[10] J. W. Freeland *et al.*, Phys. Rev. B **81**, 094414 (2010).

[11] B. R. K Nanda, S. Satpathy, and M. S. Springborg, Phys. Rev. Lett. **98**, 216804 (2007).

[12] A. Maignan, C. Martin, M. Hervieu, and B. Raveau, Solid State Commun. **117**, 377 (2001).

[13] C. He, X. Zhai, V. V. Mehta, F. J. Wong, and Y. Suzuki, J. Appl. Phys. **109**, 07D729 (2011).

[14] M. Varela, M. Oxley, W. Luo, J. Tao, M. Watanabe, A. Lupini, S. Pantelides, and S. Pennycook, Phys. Rev. B **79**, 085117 (2009).

[15] P. A. Kienzle, J. Krycka, N. Patel, and I. Sahin, REFL1D (Version 0.6.19) [Computer Software]. College Park, MD (2011)

[16] W. H. Meiklejohn and C. P. Bean, Phys. Rev. **102**, 1413 (1956).

[17] J. Nogués and I. K. Schuller, J. Magn. Magn. Mater. **192**, 203 (1999).

[18] A. E. Berkowitz and K. Takano, J. Magn. Magn. Mater. **200**, 552 (1999).

[19] V. Markovich, I. Fita, A. Wisniewski, R. Puzniak, D. Mogilyansky, L. Titelman, L. Vradman, M. Herskowitz, and G. Gorodetsky, Phys. Rev. B **77**, 054410 (2008).